

Space Science Reviews 21(1977) 309-327. All Rights Reserved.
Copyright 1977 Kluwer Academic Publishers, Dordrecht, Boston, London.
Reprinted with permission of Kluwer Academic Publishers.

This material is posted here with permission of Kluwer Academic Publishers (Kluwer). Such permission of Kluwer does not in any way imply Kluwer endorsement of any PDS product or service. Internal or personal use of this material is permitted. However, permission to reprint/republish this material for advertising or promotional purposes or for creating new collective works for resale or redistribution must be obtained from Kluwer.

By choosing to view this document, you agree to all provisions of the copyright laws protecting it.

PLANETARY RADIO ASTRONOMY EXPERIMENT FOR VOYAGER MISSIONS

J. W. WARWICK, J. B. PEARCE, R. G. PELTZER, and A. C. RIDDLE

Department of Astro-Geophysics, University of Colorado, Boulder, CO 80309, U.S.A.

(Received 24 May, 1977)

Abstract. The planetary radio astronomy experiment will measure radio spectra of planetary emissions in the range 1.2 kHz to 40.5 MHz. These emissions result from wave-particle-plasma interactions in the magnetospheres and ionospheres of the planets. At Jupiter, they are strongly modulated by the Galilean satellite Io.

As the spacecraft leave the Earth's vicinity, we will observe terrestrial kilometric radiation, and for the first time, determine its polarization (RH and LH power separately). At the giant planets, the source of radio emission at low frequencies is not understood, but will be defined through comparison of the radio emission data with other particles and fields experiments aboard Voyager, as well as with optical data. Since, for Jupiter, as for the Earth, the radio data quite probably relate to particle precipitation, and to magnetic field strength and orientation in the polar ionosphere, we hope to be able to elucidate some characteristics of Jupiter auroras.

Together with the plasma wave experiment, and possibly several optical experiments, our data can demonstrate the existence of lightning on the giant planets and on the satellite Titan, should it exist. Finally, the Voyager missions occur near maximum of the sunspot cycle. Solar outburst types can be identified through the radio measurements; when the spacecraft are on the opposite side of the Sun from the Earth we can identify solar flare-related events otherwise invisible on the Earth.

1. Introduction

1.1. SCIENCE BACKGROUND OF PRA EXPERIMENT

The phenomena of planetary radio astronomy (PRA) cover the range from broad band, black body, thermal emission to narrow band and intense coherent waves generated by energetic particles interacting with plasmas, and with each other. The details of wave-particle interaction mechanisms differ somewhat from situation to situation, but information on the physics of coherent radio emission from the planets contributes to an understanding of emissions from the Sun, stars, pulsars, and quasars. At low frequencies, typically below 40 MHz in the solar system, coherent emission tends to dominate. The study of this emission is the objective of the PRA experiment.

Table I compares Jupiter's radio emissions as they appear in different spectral ranges. The *brightness* of the emissions is conveniently described by the *brightness temperature*, T_B , an optically thick black body would have to have in order to reproduce the observed emissions. T_B also measures the average particle energy, $kT_B = E_{av}$, in this equivalent black body.

The lower right-hand entry shows that the most energetic electrons (10^8 eV) measured near Jupiter fall short by a factor of one million of being able to produce

TABLE I
Jupiter brightness temperature

f	30 000 MHz	3000 MHz	300 MHz	30 MHz
T_B	140 K	6000 K	10^5 K	10^{18} K
E_{av}	0.01 eV	0.05 eV	9 eV	9×10^{13} eV

the 30 MHz Jupiter emissions incoherently. The understanding of these non-thermal planetary radio emissions is an as yet unsolved problem in the physics of plasmas.

1.2. SCIENTIFIC OBJECTIVES OF PRA EXPERIMENT

The objectives of this experiment are:

(1) To locate and explain kilometric, hectometric, and decametric (DAM) radio emissions from the planets:

From Earth, or from spacecraft in orbit near the Earth, it has proved impossible to define precisely the position in space of planetary radio emissions from the known sources near Jupiter and Saturn. Spacecraft near the Earth have had better success in locating terrestrial kilometric sources. IMP, RAE 1 and 2, and INJUN satellites move on trajectories near or in terrestrial radio sources involved with auroral zone electron precipitation. But, the giant planets twinkle strongly at low frequencies, where interplanetary scintillations are vigorous, and prevent absolute direction-finding on a scale of the planetary diameter. The knowledge of where the source is, in space, permits correlation of other parameters, for example, *in situ* magnetic field strength and direction, plasma density, and energetic particle spectrum, pitch angles, and flux.

(2) To detect radio emissions indicative of planetary magnetic fields:

Jupiter's non-thermal low frequency radio emissions are strongly polarized, right-hand elliptical. Virtually from the instant of their discovery, 22 years ago, they have been used to infer magnetic fields of one to ten gauss on Jupiter's surface. These values are consistent with the fields measured by Pioneers 10 and 11. Our spacecraft will fly through the Solar System beyond Jupiter with a PRA experiment designed to detect radio emissions sensitively, by means of the characteristic polarizations which appear to be a signature of non-thermal emissions. Inverse square-law intensity variations of signals received during interplanetary cruise should identify each target planet's emissions and hence enable determination of magnetic field strength to within an order of magnitude. This identification does not require actual penetration of the planetary magnetosphere.

(3) To describe planetary radio emissions, and their relation to planetary satellites:

The rotation of Jupiter's magnetic field shows up in variations of radio spectrum and intensity. Surprisingly, the innermost Galilean satellite, Io, also influences the conditions for radio emission. These appear *not* to depend on the other Galilean satellites, or the closest satellite of all, Amalthea. This inconsistency may be only

apparent; the other satellites may modulate DAM emitted in directions observable only from space, or at radio frequencies below the rather high ones that can be recorded on Earth.

(4) To measure plasma resonances near the giant planets:

Wave generation in plasmas depends critically on the infinities and zeroes of the plasma dispersion equation. The spectrum observed from a spacecraft moving in such a medium shows emission cut-offs and emission 'lines' that can define plasma parameters, especially, electron density and magnetic field strength.

(5) To detect lightning on the giant planets:

Jupiter, Saturn, and even satellites with atmospheres, such as Titan, may generate lightning storms. We expect to test this hypothesis by listening for radio 'snaps' generated by lightning. Extremely useful corollary observations will be made of simultaneous light flashes in the atmosphere, and of dispersively delayed whistler mode propagation at very low frequencies.

(6) To compare radio emissions from different perspectives in space:

The non-thermal sources on Jupiter and the Sun appear to beam their emissions sharply. This inference depends on statistical studies of burst occurrence as a function of planetary (or solar) rotation. Two or more simultaneous source observations from different directions in space can be used to determine beam structure directly.

2. Physics Of Planetary Radio Sources

2.1. SOURCE LOCATION

A single phenomenon – the strong modulation of Jupiter's decametric radiation by Io leads theorists to widely divergent conclusions as to its physical mechanism. Gledhill (1967) required a disk-like sheet of plasma located in the plane of Jupiter's magnetic equator to generate DAM, as it crossed Io twice each $12^{\text{h}}55^{\text{m}}$. Radiation at the plasma frequency near Io, became DAM's source. On the other hand, Io's influence has been inferred by Goldreich and Lynden-Bell (1969) to extend along the magnetic field lines that connect it with Jupiter's ionosphere, where current instabilities generate the emission in a 'hot spot' only a few hundred kilometers across. Strong support for this model lies in the observed DAM source size, no larger than 300 km in any direction (Ratner, 1976).

These are extreme models that can be tested as the Voyager spacecraft fly past Io. Within 100 km of a radiation source on Jupiter, the signals are increased by 140 dB over their levels at Earth at *its* closest approach to Jupiter, 4.04 AU. Figure 1 shows the dynamic range of the planetary signals that can be observed from Voyager; they are normalized to the flux density seen at earth. DAM signals, if they were generated on Jupiter's ionosphere, would not show a sharp local increment as the spacecraft approaches Io. This situation may hold for certain frequency ranges and not for others, and should definitely sort out the Gledhill model as opposed to the Goldreich-Lynden-Bell model.

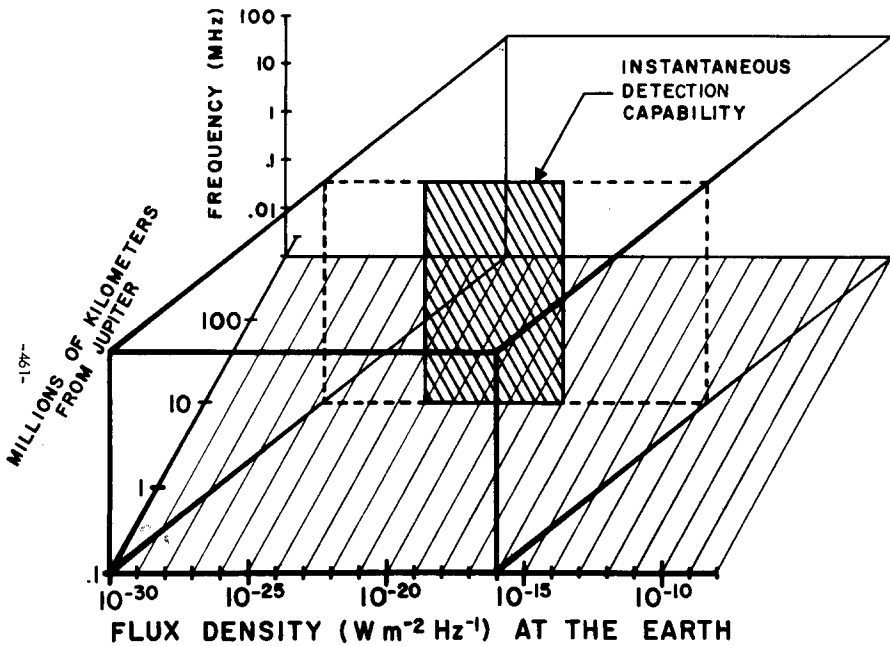


Fig. 1. The dynamic and spectral range of the planetary radio astronomy experiment. The flux density of a planetary source as it would be seen from the distance of the Earth at an assumed distance of 4.04 AU is plotted horizontally in the plane of the paper. The actual distance to the source is plotted horizontally, on the axis coming out of the plane of the paper. The frequency of observation is plotted vertically in the plane of the paper. The experiment observes over a 50 dB dynamic range at any given distance; this range can be translated by attenuators over an additional 90 dB. The experiment detects sources 80 dB weaker than it would detect at 4.04 AU, when it is 100 000 km from them. The cosmic noise lies at $10^{-19} \text{ W m}^{-2} \text{ Hz}^{-1}$ throughout the mission.

Of course, the actual situation may lie in between these extremes, and be even more complex. For example, Jupiter's auroral zones may be a source of radiation at low frequencies (Gurnett, 1976). Our data, when both feet of Io's flux tube are not visible from the spacecraft, may sort out northern and southern sources.

That the only sources of DAM radiation are Io hot spots, one in the north, the other in the south, seems unlikely. DAM, even at relatively high frequencies obviously controlled by Io, appears strongly and consistently right-handed over more than 180° of planetary longitude. The north-south symmetry of the Goldreich-Lynden-Bell model is broken only if the corresponding ionospheric magnetic fields are strongly asymmetric. Pioneer 11 data imply that Io's flux tube in the northern ionosphere has a gyrofrequency of 39.2 MHz, corresponding to 14.0 G (Acuña and Ness, 1976). The other Pioneer investigators (Smith *et al.*, 1976) imply gyrofrequencies higher by about one MHz. The observed right-hand waves correspond to extraordinary mode escape from that point. The absolute maximum of DAM recorded on Earth is 39.5 MHz. On the other hand, Pioneer 10/11 predicts a maximum of 29.1 MHz at the southern intersection. In the hemisphere opposite to where DAM reaches its right-handed frequencies of 39.5 MHz, we ought to see

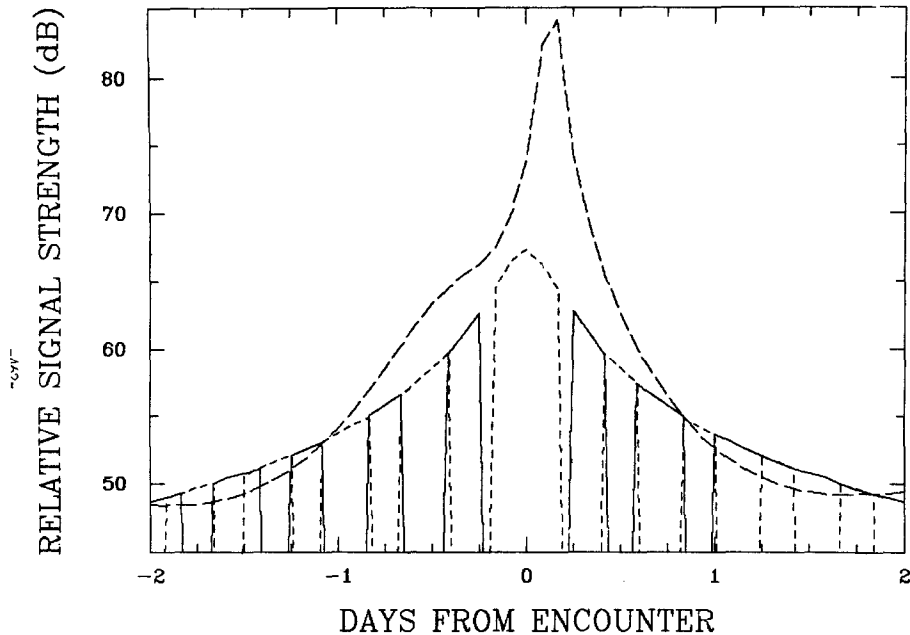


Fig. 2. Signal strength variations of radio sources at several assumed positions within the Jupiter system as seen from the JST trajectory. Continuous line: source $0.01R_j$ above northern tip of magnetic dipole; short-dashed line: source $0.01R_j$ below southern tip; long-dashed line: source centered on Io.

left-handed waves near 29 MHz. But, those longitudes emit left-handedly only below 18 MHz. The Goldreich-Lynden-Bell model, the Pioneer 10/11 extrapolations, or both, may be in error. The near coincidence of 39.5 MHz (observed upper bound to DAM) and 39.2 MHz (Io flux-tube ionospheric intersection electron gyrofrequency) is therefore probably *not* physically significant. Figure 2 compares variations in radio flux, constant at the source, seen from the trajectories of Voyager spacecraft.

2.2. CORRELATION OF RADIO EMISSIONS WITH DATA FROM OTHER EXPERIMENTS ABOARD THE VOYAGER SPACECRAFT

There is at least a possibility that one of the two Voyager spacecraft will fly quite close to Io, indeed, through the 'flux tube', the lines of force that thread Io, a few tens of thousands of kilometers from the spacecraft. On several occasions near Jupiter, both spacecraft will observe Io crossing the Gledhill magnetodisk. Data on these occasions should clarify what physical conditions are like within the observed sources of radio emission. For example, direct currents carried in and out along the two sides of the flux tube may become unstable near Jupiter. If the ionospheric intersection of the flux tube is the source of the emission, these currents can be assumed to be its energy source. A charge sheath surrounding Io also has been suggested to relate to strong electron precipitation from Io (Gurnett, 1972). If we know the values of the low energy charged particle fluxes, including pitch angle distributions, we will be able to

sharpen the emission role of electron precipitation into the 'foot' of the flux tube (e.g. its intersection with the ionosphere).

Virtually all models of the Io modulation require strong shear Alfvén waves propagated along the Io flux tube. A positive identification of these waves will constitute physical data to support models of the radio emission. But furthermore, near Io, but not within the flux tube itself, there should be present a set of strong oblique Alfvén waves, propagating into all directions from the satellite. These waves, whose properties depend on local plasma and fields, steepen, even if the propagation medium is regarded as uniform, and rapidly degenerate into hydromagnetic shock waves. Their energy tends to dissipate according to an inverse square law of distance from the satellite source region. As our spacecraft approaches Io, this wave pattern increases in power, and changes into shear waves at the close-to-Io passage of the flux tube.

Optical detection of airglow in Jupiter's auroral zones should help to identify the relationship of the kilometric Jupiter radiation (Brown, 1974) to particle precipitation. There is also the prospect of direct observation of the illuminated foot of the satellite's flux tube in the ionosphere, and its relationship to decametric radiation. Finally, Io at least, and possibly other satellites, produce atomic line emission in the UV and visible spectrum. Structure in these emissions, were it to be mapped by any of several Voyager experiments potentially capable of so doing, may refine our understanding of magnetic field line structure near the satellite, and of the geometry of the flux tube at large distances from the satellite.

3. Radio Emissions From Planets Other Than Jupiter

The polarization of Jupiter's decametric emissions suggested that Jupiter has surface magnetic fields of several gauss (Franklin and Burke, 1958). The waves turned out to be strongly right-hand elliptical or circular in polarization. It is now known that this emission is seen at the Earth predominantly when the northern end (a positive pole) of Jupiter's magnetic dipole is tipped towards us, and, as well, towards Io. The field strength in the source is probably near the local electron cyclotron frequency. Terrestrial kilometric sources (Kurth, Baumbach, and Gurnett, 1975; Gurnett, 1976) may not correspond precisely to the same mechanisms as Jupiter's, and yet there is a rough correspondence between terrestrial polar emissions near 200 kHz, and terrestrial magnetic fields in the same spatial regions (Kaiser and Stone, 1976). The discovery of radio emissions from Saturn near one or two MHz frequencies (Brown, 1975) suggests polar fields of one or two gauss on that planet. A separate analysis of data from the Radio Astronomy Explorer satellite in orbit around the Moon (Kaiser, 1977) is now under way. Measurements from the Voyager spacecraft as they approach Saturn will confirm and further refine this result.

Radio emissions provide a way to estimate strengths of magnetic fields at great distances from the planets. This is a satisfactory substitute for detailed *in situ* field measures only when the latter are impossible, as for example when radiation hazards

(at Jupiter) make close fly-bys difficult, or when spacecraft survival (through the rings of Saturn) necessitates remote periapses.

Warwick (1976) provides a deductive theory to predict what fields are like on the outer planets. Warwick modified Malkus' precessional dynamo theory (1963, 1968) for the terrestrial field, and compared it to Solar System dynamos in the Sun, Mercury, and Jupiter. Extended to Saturn, the theory predicts a field driven by the satellite Titan; Neptune's field, similarly, is driven by Triton. However, Uranus is too far from the sun to precess strongly under the solar couple, and experiences no precession from its satellite. The Uranus polar field, produced by the weak solar couple acting on Uranian J_2 , should be two orders of magnitude less than Saturn's field. Neptune's polar field is like Jupiter's polar field. Triton orbits close to Neptune, and might be another Io in respect to DAM.

Saturn, Uranus, and Neptune should possess polar fields of 5, 0.03, and 17 G, respectively. Of course, the very weak precessional effect at Uranus provides a critical observational test of the precessional theory of planetary magnetism: the presence of strong fields there as well as on Neptune would imply either that the Uranian satellites do not lie sufficiently close to the planetary equator (in which case Malkus' idea might still survive) or that planetary dynamos are forced by thermal convection alone (Rochester, Jacobs, Smylie, and Chong, 1975). At Uranus, PRA should receive Neptune's radio emissions fairly strongly.

4. The Phenomenology Of Planetary Radio Emissions

Two planets certainly, and possibly also Saturn, are known to produce non-thermal radio emissions. At the Earth a strong connection exists between auroral zone electron precipitation, auroral arcs seen with photometers, and terrestrial kilometric radiation. Terrestrial radio spectra do not show the same tight geometrical relation between emission frequency and propagation direction as does Jupiter. On the other hand, Jupiter's emissions in the hectometric and kilometric range may more closely resemble the terrestrial kilometric emissions.

Jupiter's DAM emission, observed at the Earth, precisely defines the orientation of Jupiter's magnetic dipole, and the position of Io in its orbit. A two dimensional plot of DAM as a function of Io's terrestrial longitude in its orbit and Jupiter's sub-terrestrial zenomagnetic longitude defines a precise, stable asymmetric pattern (see Figure 3). The figure also shows DAM plotted once more, but with Europa's longitude in its orbit with respect to superior geocentric conjunction in place of sub-terrestrial zenomagnetic longitude. The object of this graph is to demonstrate the strong dominance of the Io control over DAM, as compared with putative Europa control. Io and Europa are close to two-to-one commensurability in their orbital frequencies, which makes a sample of DAM data based on Europa longitudes show virtually the same kind of effects as does one based on Io longitudes. The diagonal patterns on this graph can be used to define the period of Europa relative to Io. In these 16 years of data the occurrence probability on Io-Europa coordinates

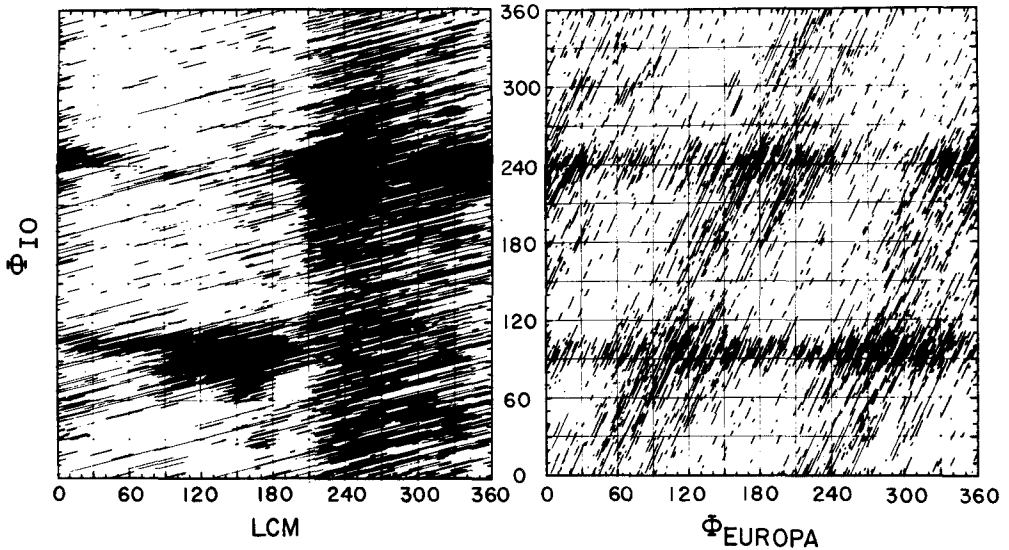


Fig. 3. Observing time lines during Jupiter emission events recorded at Boulder, Colorado, 1960 to 1974. The left-hand half of the figure plots longitude of Jupiter's central meridian ($\lambda_{III}(1965.0)$) as 'LCM' on the horizontal scale; the right-hand half plots longitude of Europa from superior geocentric conjunction as Φ_{Europa} on the horizontal scale. The vertical scale is the corresponding Φ_{Io} .

depends more on the near commensurability than on Io or Europa acting independently. If Europa had acted independently of Io its control would have appeared as a vertical region of enhanced probability of occurrence on this graph.

But these figures are based on ground level data, and necessarily refer to radio frequencies above say 5 or 10 MHz. From data taken in space near the earth, plots of this sort have been extended to lower frequencies (Carr and Desch, 1976), but do not yet reveal unambiguously controls by Europa or the other Galilean satellites. To create any of these diagrams requires a great many data. To sort out Io and Europa necessitates uniform data coverage over the Io-Europa plane, which requires even more data. From our spacecraft nearer to Jupiter, and with our experiment more sensitive to DAM at all frequencies up to 40 MHz, we hope to construct these plots adequately within one year's time during cruise towards and away from Jupiter. In particular, the 24-hour periodicity bias in the Earth-based data will not be present. Also, we will reach zenographic latitudes differing by a significant amount from the $\pm 3^\circ$ seen from the Earth.

5. The Relation Between Radio Spectra and Plasma Dispersion Equations

In the simplest description of a plasma, only cold electrons of density N_e per cm^3 are present in otherwise empty space; no magnetic field exists. Then, the wave index of

refraction n relates to N_e by the familiar Eccles relation $n^2 = 1 - x$, where $x \equiv 4\pi N_e e^2 / m\omega^2$, where e is the electron charge, 4.80×10^{-10} esu, m is its mass, 9×10^{-28} g, and ω is the 'circular' wave frequency, $2\pi f$, in radians s^{-1} . Wave propagation cuts off entirely for $\omega \leq \omega_p = \sqrt{4\pi N_e e^2 / m}$, the plasma, or Langmuir, frequency. Waves created where $\omega > \omega_p$ reflect or refract from spatial regions where $\omega \leq \omega_p$. Extensive volumes exist beyond which sources are invisible. Such effects appear in data on terrestrial and solar radio emissions. As $N_e \rightarrow 0$, or $\omega \rightarrow \infty$, $n^2 \rightarrow 1$, and the relation describes a free-space EM wave.

Suppose the plasma electrons are hot; then to a crude approximation, in addition to the mode described above, a second mode $n^2 = (c^2/v_{th}^2)(1 - x)$ appears, where c = the velocity of light and $v_{th} = \sqrt{2kT/m}$, the thermal speed of electrons in the plasma. This mode is the plasma, or Langmuir, wave mode, whose phase velocity, for wave frequencies greater than the plasma frequency, approaches thermal speeds. These waves can be resonantly generated through the action of fast streams of electrons, protons, or other charged particles moving at the phase velocity. This mechanism creates emissions above the plasma frequency; polarized longitudinally, they do not propagate into free space. However, coupling of two such plasma waves, or their propagation against a density gradient, can excite EM radiation 'freely' propagating along the Eccles branch. For example, coherent decametric radio emission is created in this way by the Sun.

Further complications arise when the plasma is embedded in a static magnetic field. For propagation along the lines of force the freely propagating mode splits into two modes. Each connects onto the plasma wave mode. There results $n^2(\omega)$ curves with, in general, three branches at a given wave frequency. One of these modes has a zero below $x = 1$, at $x = 1 - y$ (where $y < 1$), and at $x = 1 + y$. The root $1 - y$ disappears where $y > 1$. $y \equiv \omega_{ge}/\omega$, ω_{ge} = the electron gyrofrequency. Two of the branches connect to free space; when $y < 1$, the branch with a zero at $x = 1 + y$, which contains the low phase velocity portion of the dispersion diagram, does *not*. Mode coupling near $x = 1$ is therefore often required for generation of escaping waves generated in this mode. Near the point $y = 1$, but for low plasma density, the index of refraction as a function of frequency consists of three modes, as usual; for one of these modes, n is singular. The electron gyrofrequency is therefore a 'resonance' frequency of the plasma, and, like the plasma wave mode, represents waves that can be generated by wave-particle interactions. Like plasma waves, the energy in the gyro resonance mode escapes only through mode coupling. This resonance occurs for waves polarized in the extraordinary mode. Wave polarization therefore helps to identify the mechanisms of generation and escape.

Finally, the dispersion relation can exhibit resonances at the *ion* gyrofrequency. It seems unlikely that this resonance has to do with DAM; at low enough frequencies it may nevertheless lead to some observables. For propagation across the lines of force, the simple resonances at ion and electron gyrofrequencies combine in algebraically more complicated ways to create 'upper' and 'lower' hybrid resonances.

6. Lightning Detection

Clouds on earth, especially cumulo-nimbus structures, create electric charge separations measured in tens of coulombs over hundreds or thousands of meters distance, and localized field strengths of tens of kilovolts per meter. This mechanism is in many ways still mysterious, and may depend on the residual ionization of the air created by radioactivity in rocks and soil and by cosmic rays. Air breakdown occurs as these enormous amounts of electric charge travel from cloud to ground, or cloud to cloud; during this process air is heated to temperatures of tens of thousands of degrees absolute. The formation of raindrops, or ice crystals, in clouds can conceivably create the charge separations on a microscopic scale; however, the dynamics of convective transport and concentration of these charges within localized portions of clouds is not understood.

Without stressing the *differences* between Earth and the giant planets, we can reasonably presume that at least several ingredients of the terrestrial electrostatic machine are also present in the latter's atmospheres. Even Titan has been suggested to generate lightning.

A lightning stroke can be regarded as a short dipole antenna at fundamental frequencies associated with the lightning return. These are in the order of $(0.1 \text{ millisecond})^{-1}$, and create most of their radiation in the VLF range, typically at 10 or 20 kHz. They also generate radiation at much higher frequencies, into the lower VHF range, and strongly at the frequencies of the Voyager radio astronomy receiver. This decametric emission occurs during formation of the lightning 'leader', when negative charge is usually lowered to ground.

At extremely low frequencies, the lightning radio energy tunnels through our ionosphere and propagates dispersively along the lines of force of our magnetosphere. For a receiver within the direct, straight-line propagation path from a stroke, the sequence of events is a snap, followed at several seconds by a whistler descending in tone through the audio range.

At giant planets like Jupiter, we may expect to record the time of a stroke via its radio emission at decametric wavelengths, and, several tens of seconds later, the dispersed and refracted low-frequency components at ELF or VLF. We should compare our data at these times with the plasma wave receiver and with photopolarimeter data. In view of the widespread supposition that lightning occurs elsewhere than just on Earth, we will operate our receiver in the high-speed data recording modes that most easily can identify lightning strokes at Jupiter and Saturn.

7. Directivity Patterns Of Radio Emissions From the Sun and Planets

Figure 4 illustrates the variations of DAM as Jupiter rotates and Io revolves; these are profiles each of which is constructed on the basis of all data within a given observing year, called an 'apparition'. Fifteen years of data are represented here, that

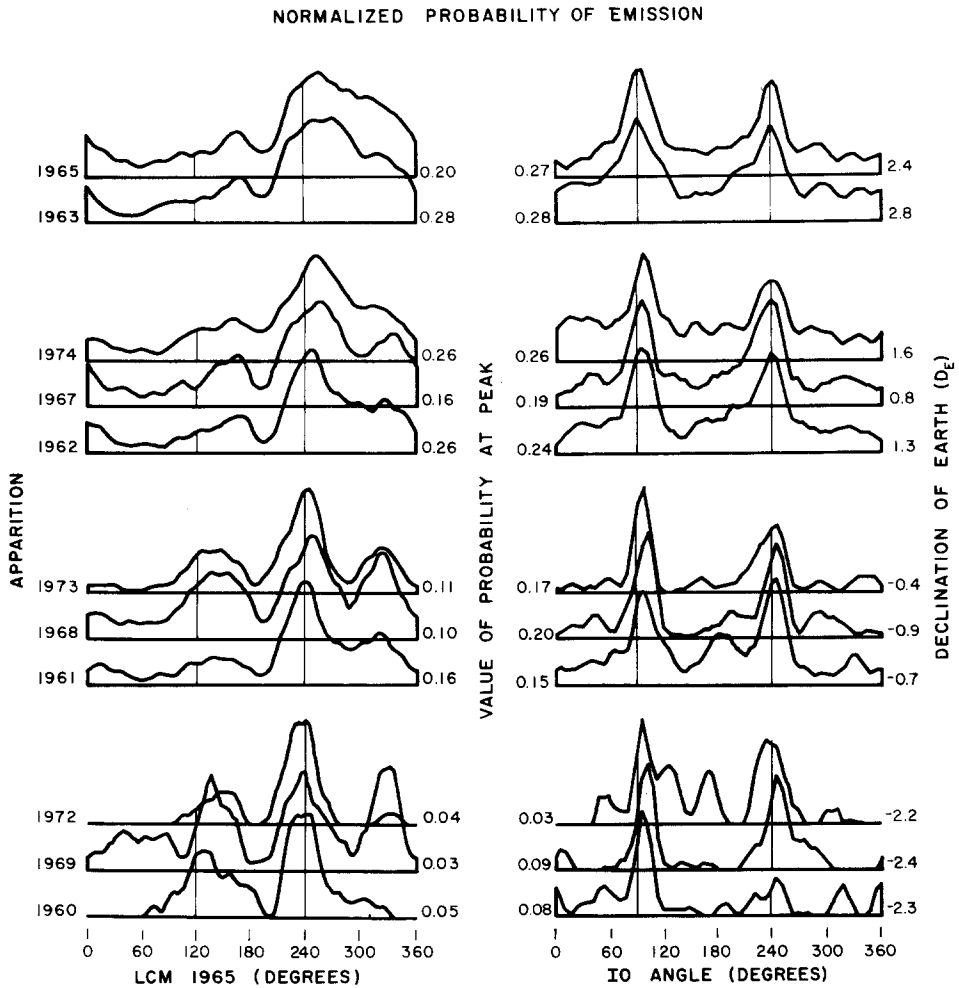


Fig. 4. Longitude histograms of Jupiter's decametric emission plotted with respect to magnetic axis orientation (left-hand set of figures) and Io's longitude (right-hand set of figures). The data are further sorted according to the tilt angle between Jupiter's rotation axis and the perpendicular to the ecliptic.

cover the frequency range from 7.6 to 41 MHz. The years are sorted into groups of three; each group contains all the apparitions out of the fifteen during which the tilt of Jupiter's rotation axis had the value called 'declination of earth (D_E)'. The curves are plotted on different vertical scales, with a constant height. The corresponding peak probability is shown alongside each curve.

The years immediately after the sunspot maximum in 1957 were notorious for low probability of DAM occurrence. The same phenomenon occurred again 11 or 12 years later, in 1969 and subsequently. This coincidence of DAM probability and the sunspot cycle is today recognized as an association with the revolution period of Jupiter around the Sun, rather than the 11-year solar activity cycle. The purpose of Figure 4 is to demonstrate the nature of this association.

The total range of D_E values does not quite reach 6° . Since the rotation of Jupiter's magnetic field creates the LCM profiles shown in Figure 4, and since this field is inclined at an angle of 10° to the rotation axis of Jupiter, we must ask how the 6° rotation axis tilt range can appear so strongly against the much larger dipole axis tilt range. In other words, zenomagnetic latitudes from $+13^\circ$ to -7° are involved in the emission during the years of maximum emission probability; latitudes of $+7^\circ$ to -13° are involved during the minimum. Despite the overlap in latitude range, this small difference changes emission probability by factors of five or more. This implies that DAM is highly directive, within angles of only a few degrees.

It seems that Jupiter's magnetic field is clearly not symmetric between the northern and southern magnetic hemispheres, and the asymmetry is much sharper than the small asymmetry detected by Pioneer 10/11 (*loc. cit.*). Aboard the Voyager spacecraft, the radio receivers will observe DAM over a magnetic latitude range significantly different from what is seen at the earth, in terms of a very few degrees.

Different rotational profiles are observed at different values of D_E . Ten years data suffice to define the basic rotation period to within about 0.05 s; this corresponds to a longitude error in one rotation of about $\pm 5^\circ$. Yet another determination of rotation rate depends on the comparison of individual radio spectrum observations made during a given rotation, with similar observations over intervals of 10 or 15 years. The complex patterns of dynamic development on these spectra are strikingly similar even over this long an interval, and can be compared to less than $\pm 10^\circ$ of longitude.

The beaming of the emission is therefore evident in data taken on the Earth, but requires intercomparison of events at widely different times of occurrence. From each spacecraft, we achieve different angular relations to the sources of emission than those simultaneously perceived from the Earth. A given emission event should therefore appear differently from these perspectives; its geometrical beaming can be defined more accurately.

An unplanned benefit of these spacecraft on interplanetary cruise derives from the fact that they will at six months intervals be situated on the opposite side of the Sun from the Earth. The receivers are capable of detecting and identifying solar outbursts associated with solar flare activity not visible from the Earth. On board, there are other particles and fields experiments that can observe, for example, energetic electrons and protons produced in these events. A long-standing problem in solar physics will be clarified on the basis of these data which can be compared with ground-based and circumterrestrial data taken at the same time: what are the propagation paths to Earth of energetic protons from flares on the opposite side of the Sun?

Solar radio emissions are also strongly directive, though less so than DAM from Jupiter. Their emission patterns are measured in many tens of degrees, and are defined not only by the physics of emission generation, but also by propagation through the solar corona. The Voyager missions encompass the time of forthcoming solar maximum, and should therefore be rich in solar radio events.

8. Instrument Description

The planetary radio astronomy receiving system was conceived and designed functionally by an investigator group of 12 scientists* and a PRA project office consisting of the four authors of this paper.

Conceptually the receiver is designed to detect planetary emissions by way of their characteristic polarization. Jupiter, the only planet whose radio polarization is known, emits strongly polarized waves in the right-hand elliptical or circular mode at DAM frequencies above 15 or 20 MHz. Earth-based observations (from 4 AU) are generally swamped by cosmic radio waves coming from all directions over the sky. Only a sharply beamed receiving antenna can possibly isolate the planetary signals from the sky background, and yet our spacecraft are much too small to accommodate the large antenna arrays that would be necessary for direct detection. Jupiter's signals, received on an Earth-based omni-directional antenna, roughly amount to a maximum of about 10% of the cosmic background at almost all frequencies over the range of hectometric and decametric wavelengths. However, this background is virtually unpolarized; it therefore offers a way to separate planetary signals. We will observe right-hand and left-hand polarized signals in separate channels. Most of the Jupiter signals will lie in the right-hand channel only. The cosmic noise and, as well, most solar emission, will fall equally into the two channels. The difference in power, right-hand minus left-hand, should therefore be a positive number representing substantially all of the Jupiter signals at frequencies above 20 MHz.

As the spacecraft approach to about one AU from Jupiter, the perceived planetary signals will increase to about the same strength as the cosmic flux; within that distance of the planet, they will eventually greatly exceed the cosmic background. This is shown by Figure 1, in which the cosmic noise flux density is close to $10^{-19} \text{ W m}^{-2} \text{ Hz}^{-1}$, and, of course, is invariant throughout our mission. The equivalent (terrestrially perceived) planetary flux density we can record at various distances from the source is shown, and of course greatly exceeds the range of flux densities recordable at the Earth. The most critical technical problem in the realization of a receiver to accomplish these records has been the extremely broad dynamic range necessary for measuring the weakest signals, $10^{-30} \text{ W m}^{-2} \text{ Hz}^{-1}$ (normalized to the

* James W. Warwick	Principal Investigator	University of Colorado
Joseph K. Alexander	Deputy P-I	Goddard Space Flight Center
André Boisshot	Co-I	Paris Observatory
Walter E. Brown, Jr.	Co-I	Jet Propulsion Laboratory
Thomas D. Carr	Co-I	University of Florida
Samuel Gulkis	Co-I	Jet Propulsion Laboratory
Fred T. Haddock	Co-I	University of Michigan
Christopher C. Harvey	Co-I	Paris Observatory
Yolande LeBlanc	Co-I	Paris Observatory
Robert G. Peltzer	Co-I and Project Eng.	University of Colorado
Roger Phillips	Co-I	Jet Propulsion Laboratory
David H. Staelin	Co-I	Massachusetts Institute of Technology
Glenn Lockwood	Co-I (resigned)	Communications Research Center, Canada

distance of the Earth) in the presence of very strong ones, $10^{-18} \text{ W m}^{-2} \text{ Hz}^{-1}$. And, this dynamic response must hold at the front end of the receiver, where no attenuation is possible if these weakest signals are to be measured. The receiver as constructed achieves about 65 dB of undistorted dynamic range in the presence of an out-of-band signal.

Planetary coherent emission, again with Jupiter as our best-known example serving as a model, covers frequencies all the way from kilometric to decametric wavelengths. The latitudes actually achieved by Voyager at Jupiter will be somewhat higher than the values we ever see from the Earth. Nevertheless, we have assumed that about 40 MHz (upper limit observed at Earth) is as high as required for studies of DAM, and this sets the upper frequency limit of our receiver. On the side of low frequencies, Jupiter emission has not been positively detected much below 300 kHz (one kilometer wavelength). Terrestrial emissions, however, smoothly continue from frequencies near that value down to the frequencies characteristic of trapped waves within the magnetosphere, which exist as low as a few hertz. The major thrust of the PRA experiment, however, is to study the freely-propagating waves generated in planetary plasmas, and these waves are not obvious below a few tens of kilohertz. To observe planetary waves anywhere in this extensive range from broadcast frequencies (hundreds of kilohertz) down to very low frequencies (tens of kilohertz) will be difficult from Voyager on account of the strong spacecraft power supply signature we expect to be present throughout this low-frequency range. To help us succeed, we have designed the receiver to observe *between* successive harmonics of the spacecraft power subsystem, which is a 50 V, square-wave switched, 2.4 kHz supply. The receiver's local oscillator is phase-locked to the spacecraft clock that controls the frequency of this supply.

The power supply switching speed is basically a few microseconds. This implies that at some frequency in the broadcast band there will be a sharp roll-off in spacecraft interference; however, various other spacecraft subsystems use faster logic, which can introduce interference that does not follow this pattern. On Voyager, the spacecraft engineers have tried to identify some of these subsystems, and reduce their deleterious impact on the radio astronomy experiment. Furthermore, there is an over-all spacecraft requirement for electrostatic shielding to control spacecraft charging phenomena in magnetospheric environments. This shield provides significant radio frequency shielding as well.

In order to observe at low frequencies, we have implemented an LF-band receiver with a bandwidth of 1 kHz precisely centered between the spacecraft's power supply harmonics. There are 70 discrete observing frequencies ranging from 1.2 kHz to 1.228 MHz which are spaced at 19.2 kHz intervals. At high frequencies, we use an HF-band receiver, with a bandwidth of 200 kHz spaced in 307.2 kHz intervals at 128 points from 1.228 MHz to 40.5504 MHz. The basic mode of the instrument is a 6-sec scan from 40.550 MHz to 1.2 kHz during which the receiver dwells at each frequency for a total of 30 millisc. This totals 198 frequency points; two additional points are filled with 'housekeeping' data describing the experiment's status.

The sensitivity requirements of the instrument are set by the basic radiometer formula: $\Delta S/S \sim (B\tau)^{-1/2}$, where ΔS is the fluctuation in received total flux S that occurs when noise in the bandwidth B is detected and smoothed with a time constant τ . This ratio is $\Delta S/S \sim 1 \times 10^{-2}$ in the HF range and $\Delta S/S \sim \frac{1}{5}$ in the LF range. The receiver alternates right-hand and left-hand polarization measurements at successive frequency dwell points as it steps through the scan range. Any polarized planetary emission whose flux exceeds S by an amount ΔS , therefore will be detected at the one sigma level in a comparison between adjacent channels spaced 307.2 kHz apart, and observed within 60 millisecond. S , the total flux, is, at these low frequencies, entirely dominated by the cosmic radio noise. As a result, we can expect to observe planetary emissions whose flux density is $\sim 10^{-21} \text{ W m}^{-2} \text{ Hz}^{-1}$ in the HF range, and $\sim 2 \times 10^{-20} \text{ W m}^{-2} \text{ Hz}^{-1}$ in the LF range.

The sequence of receiver configurations is controlled by the Voyager flight data system, which is prepared to handle a normal maximum of 267 bits per second from the radio astronomy receiver. In addition to the above frequency scan, the receiver can be commanded to receive data on a single frequency, or pair of frequencies in right-hand and left-hand polarization; it can be directed to calibrate itself internally, a calibration that can in turn be calibrated against the constant cosmic noise levels we expect to observe throughout the mission; it can be directed into special modes in

TABLE II
Instrument Performance parameters

Parameter	LF Band	HF Band
Frequency range	1.2 kHz to 1.3 MHz	1.2 MHz to 40.5 MHz
Frequency steps	70	128
Step increment	19.2 kHz	307.2 kHz
IF Bandwidth	1 kHz/800 Hz at -3 dB	200 kHz at -3 dB
	1.2 kHz at -90 dB	900 kHz at -55 dB
Sensitivity	$0.3 \mu\text{V}/\sqrt{(\text{kHz})}$	$0.1 \mu\text{V}/\sqrt{(\text{kHz})}$
Polarization discrimination	20 dB	
Frequency stability	10^{-5}	
Commandable attenuation	0-90 dB in 15 dB steps	
Logarithmic dynamic range	Dual slope, 50 dB	
Overall dynamic range	140 dB	
Input impedance	$22 \text{ M}\Omega + 12 \text{ pF}$	
Postdetection time constant	25 ms, 0.1 ms in high data rate mode	
Data rate	266 bps max in low data rate mode	
	115.2 kbps in high data rate mode	
Frequency range scan time	6 seconds	
Calibrator	3 levels + off (1.2 kHz to 40.5 MHz)	
Operating modes	6 primary	
Power	6.7 W (2.4 kHz, 50 V square wave)	
Radiation tolerance	5×10^{12} electrons/cm ² minimum	
Operating life goal	4 years in space environment	
Temperature range	-30 to 85 °C	

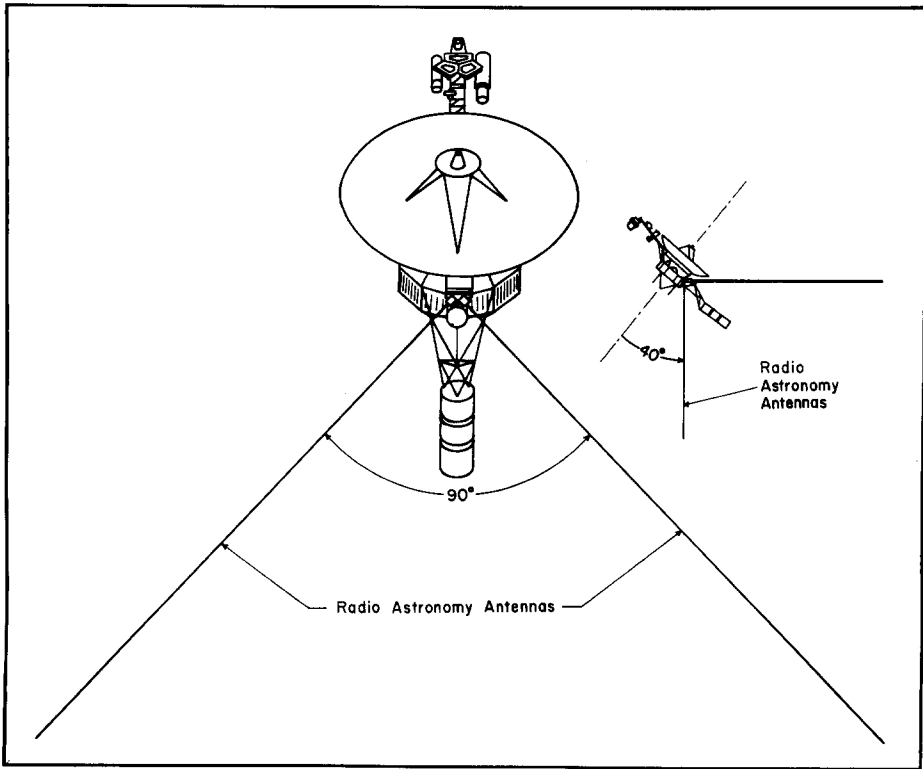


Fig. 5. The planetary radio astronomy experiment antenna geometry. The large picture is oriented so that the magnetometer boom points directly out of the plane of the paper. The smaller figure is a side view of the spacecraft, rotated 90° .

which the very high bit rates nominally assigned to the Voyager imaging subsystem (115 kilobits per second) are instead dedicated for brief observation periods to the radio astronomy receiver; we can operate usefully with extremely low bit rates, as low as 0.01 or 0.1 bits per second, where the instrument becomes in effect a single frequency radiometer with extremely long integration times; and finally, the receiver can be commanded to observe at the exact frequencies of the spacecraft power sub-system in the LF range.

Table II describes over-all performance parameters that have been achieved with the delivered receivers. The details of the design and construction* of these receivers are reported by Lang and Peltzer (1977). A note is required with respect to the polarization discrimination entry, 20 dB. This performance is demonstrably achieved within the receiver proper; however, the combination of the receiver plus antenna system falls short of this value, mainly because the electromagnetic performance of the pair of 10-m monopoles loaded against the spacecraft conductive structure is not the ideal polarization purity which would be obtained from a pair of

* The development and construction of the receiver was accomplished by the Martin Marietta Corporation (Denver Division) under a contract with the University of Colorado.

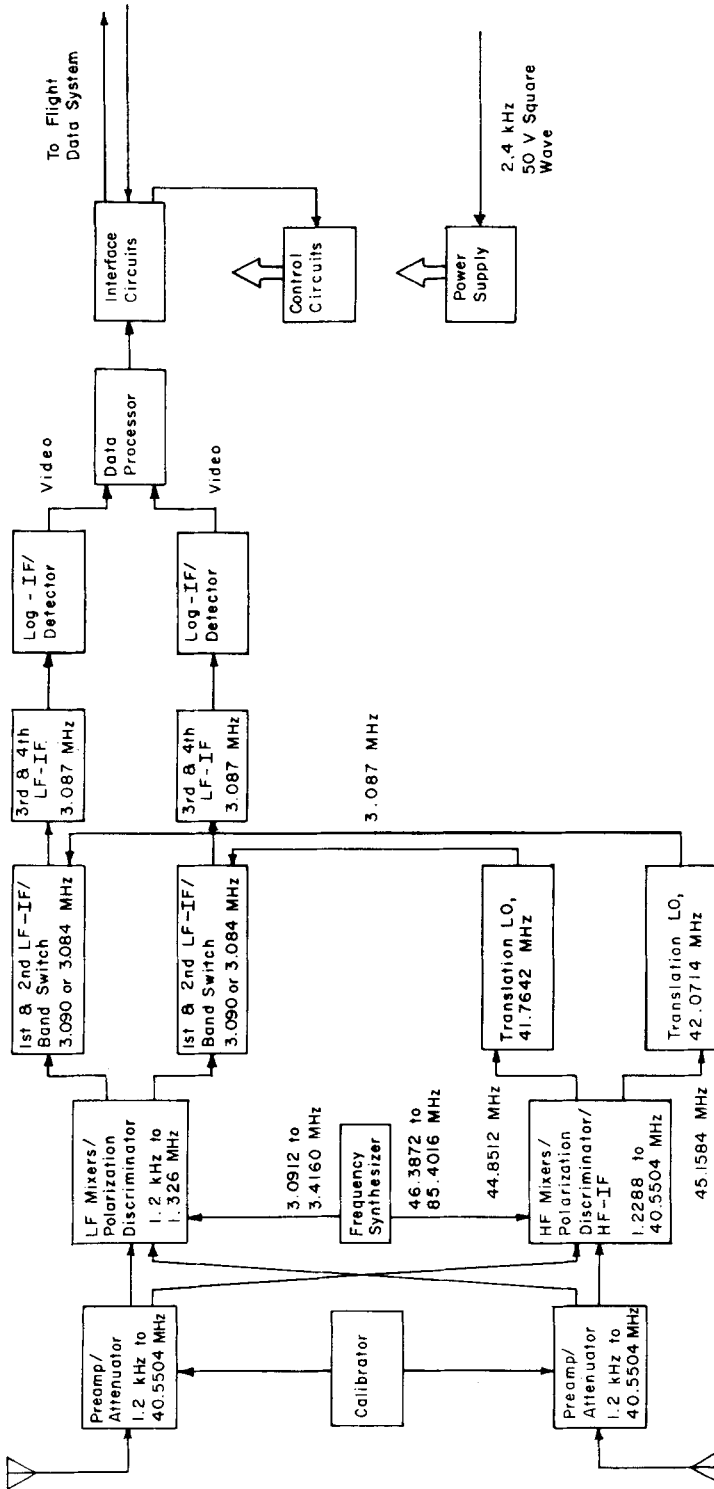


Fig. 6. Simplified block diagram of the planetary radio astronomy receiver. Connections between the antennas and the plasma wave experiment are not shown.

orthogonal dipoles. Furthermore, during the mission, the various planetary emission sources lie in directions that move within our antenna geometry. Even if the polarization reception were completely ideal along the direction perpendicular to our orthogonal monopoles, the right-hand/left-hand separation would be less than ideal for every other direction in space. Figure 5 shows the physical orientation of the antenna system on the spacecraft. Figure 7 shows how polarization varies along the JST trajectory. An attempt has been made to assign correct values for the orientation of the equivalent electric dipole formed by each monopole individually loaded against the actual spacecraft.

Figure 6 shows the functional block diagram of the receiver, with a detailed frequency layout. The HF-band receiver is a dual conversion superheterodyne system, which uses the LF band IF strip after the second conversion. The synthesizer is a digitally controlled local oscillator which is locked to the 2.4 kHz spacecraft clock. The data processor converts the signals from the log IF/detector strips into 8-bit words. The word size, it should be noted, permits a scale step size of about

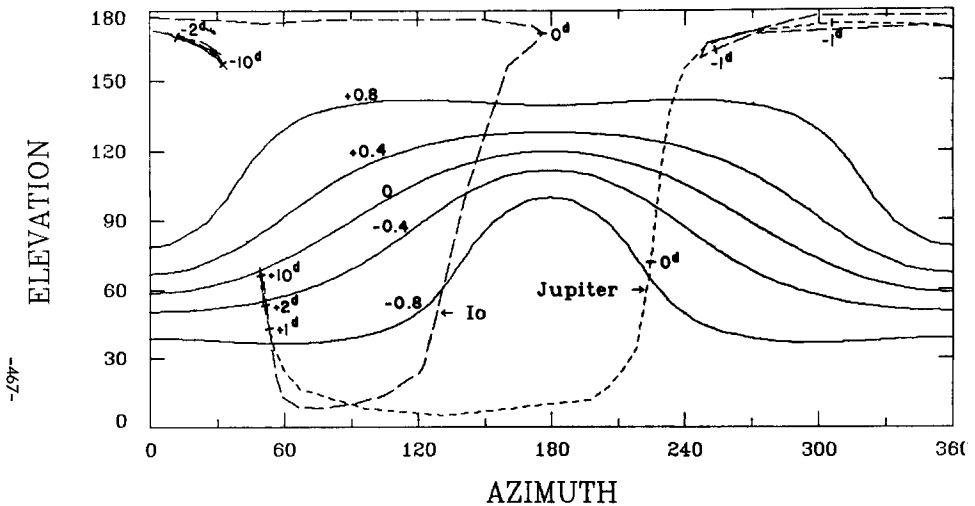


Fig. 7. The polarization performance of the planetary radio astronomy experiment antennas during the JST trajectory. The coordinates are spacecraft azimuth and elevation. The continuous curves show the fractional polarization, $(P_R - P_L)/(P_R + P_L)$, that will be recorded from a fully polarized, right-hand circular source at each azimuth and elevation. These curves are based on both scale model measurements and theoretical calculations using the detailed spacecraft geometry. The dashed curves represent the spacecraft coordinates of Io and of Jupiter throughout the JST trajectory.

0.1 dB to be measured. This measurement accuracy allows detection of planetary signals that are 20 dB below the cosmic noise when the cosmic noise flux lies on the 10 dB scale step.

References

- Acuña, M. H. and Ness, N. F.: 1976, in T. Gehrels (ed.), *Jupiter*, University of Arizona Press, Tucson, p. 836.
- Brown, L. W.: 1974, *Astrophys. J.* **194**, L159.
- Brown, L. W.: 1975, *Astrophys. J.* **198**, L89.
- Carr, T. D. and Desch, M. D.: 1976, in T. Gehrels (ed.), *Jupiter*, University of Arizona Press, Tucson, p. 693.
- Franklin, K. L. and Burke, B. F.: 1958, *J. Geophys. Res.* **63**, 807.
- Gledhill, J. A.: 1967, *Nature*, **214**, 155.
- Goldreich, P. and Lynden-Bell, D.: 1969, *Astrophys. J.* **156**, 59.
- Gurnett, D. A.: 1972, *Astrophys. J.* **175**, 525.
- Gurnett, D. A.: 1976, in B. M. McCormac (ed.), *Magnetospheric Particles and Fields*, D. Reidel, Dordrecht, Holland, p. 197.
- Kaiser, M. L. and Stone, R. G.: 1975, *Science*, **189**, 285.
- Kaiser, M. L.: 1977, *Astrophys. J.* in press.
- Kurth, W. S., Baumbach, M. M., and Gurnett, D. A.: 1975, *J. Geophys. Res.* **80**, 2764.
- Lang, G. J. and Peltzer, R. G.: 1977, *Planetary Radio Astronomy Receiver*, *IEEE Transactions on Aerospace and Electronics Systems*, submitted for publication.
- Malkus, W. V. R.: 1963, *J. Geophys. Res.* **68**, 2871.
- Malkus, W. V. R.: 1968, *Science*, **160**, 259.
- Ratner, M. L.: 1976, 'Very-Long Baseline Observations of Jupiter's Millisecond Radio Bursts', Thesis, Boulder: University of Colorado, unpublished.
- Rochester, M. G., Jacobs, J. A., Smylie, D. E., and Chong, K. F.: 1975, *Geophys. J. Roy. Astron. Soc.* **43**, 661.
- Smith, E. J., Davis, L. Jr., and Jones, D. E.: 1976, in T. Gehrels (ed.), *Jupiter*, University of Arizona Press, Tucson, p. 806.
- Warwick, J. W.: 1976, in B. M. McCormac (ed.), *Magnetospheric Particles and Fields*, D. Reidel, Dordrecht, Holland, p. 291.